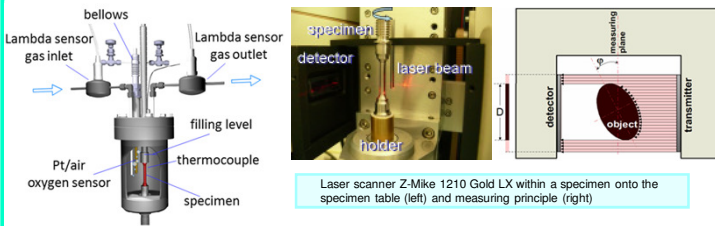


Motivation

Intensive study of ferritic and ferritic/martensitic oxide dispersion strengthened (ODS) steels has arisen with increased interest in these materials as candidates for application in nuclear power plants of 4th generation and for fusion reactors. High-temperature strength obtained due to randomly dispersed, fine second-phase particles in a metallic matrix by powder metallurgy process broadens the application range with respect to temperature. Strengthening mechanisms such as precipitation hardening and solid solution strengthening become more derivative for the fine dispersoids in comparison to conventional steels. The properties of ODS steels are strongly influenced by the production route, in addition to chemical composition leading to formation diverse structural compositions or bimodal structures.

Ferritic 12Cr- and 14Cr-ODS steels produced by powder metallurgy technique in form of plates and bars, respectively, are studied with respect to creep-to-rupture behavior in stagnant, oxygen-controlled lead ($c_{O_2} = 10^{-6}$ mass-%) at 650°C. Similar experiments were performed in air so as to understand the effect of liquid metal on creep.

CRISLA Facility and Materials



Five capsules with liquid lead (900 ml)
Three capsules with air (230 ml) for reference tests

Determination of the creep-rupture parameters:

$$Lr = Lc + 2 \sum_i [(D/d_i)^{2n} t_i]$$

$$\epsilon_r = \Delta L / L_r \times 100; \quad \epsilon_{r,R} = \Delta L_r^R / L_r \times 100$$

Creep-rupture specimen

Table 1: Composition (in mass%) and heat treatment of the extruded 12Cr-ODS plates

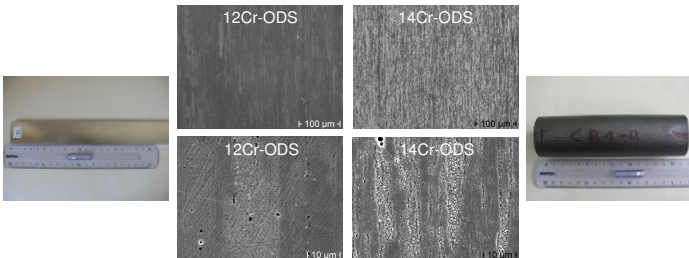
Chemical composition														Calculated	
C	Si	Mn	P	S	Ni	Cr	W	Ti	Y	O	N	Ar	Y ₂ O ₃	O	
0.02	0.02	<0.01	<0.005	0.002	<0.01	12.2	1.94	0.25	0.17	0.12	0.01	0.005	0.22	0.08	

Thermal heat treatment: hot extrusion at 1150°C, with following forging at 1150°C; finally cold rolling up to 40% reduction and re-crystallized at 1150°C for 1 h.

Table 2: Composition (in mass%) and heat treatment of the cold worked 14Cr-ODS bars

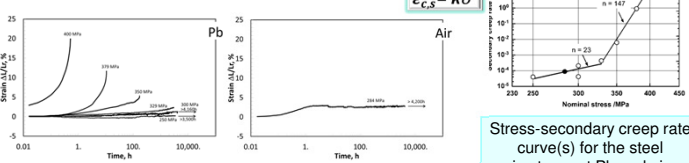
C	Si	Mn	Cr	W	Ti	Y	O
0.41	0.32	0.28	13.46	0.88	0.39	0.22	0.29

Thermal heat treatment: 1050°C for 1.5 h



Creep-Rupture Characteristics

12Cr-ODS Steel



Strain-vs.-time curves for the steel in stagnant Pb and air

Table: Creep-to-rupture characteristics of the steel in stagnant Pb at 650°C

σ MPa	t_R h	$\epsilon_{r,R}$ %	Z %	$\dot{\epsilon}_{c,s}$ %/h	$t_{1,2}$ h	$t_{2,3}$ h
400	0.52	22	42	25.0	0.2	0.18
379	10.6	18	44	0.90479	1.2	9.05
350	170.2	11	30	0.006275	62.9	113.2
329	2,982.4	6	17	0.000432	471	2,982.3
300*	>2,100	-	-	0.0002064	320	-
300*	>4,160	-	-	0.0000418	615	-
250*	>3,500	-	-	0.0000398	191	-

* - stopped
* - running

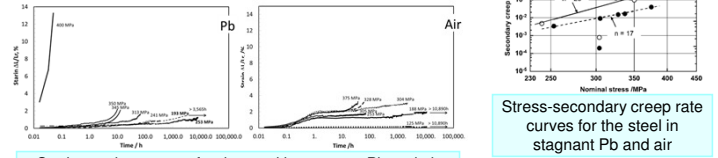
Table: Creep-to-rupture characteristics of the steel in stagnant air at 650°C

σ MPa	t_R h	$\epsilon_{r,R}$ %	Z %	$\dot{\epsilon}_{c,s}$ %/h	$t_{1,2}$ h	$t_{2,3}$ h
284*	>4,200	-	-	0.000088	1.23	-

* - running

Creep-Rupture Characteristics

14Cr-ODS Steel



Strain-vs.-time curves for the steel in stagnant Pb and air

Table: Creep-to-rupture characteristics of the steel in stagnant Pb at 650°C

σ MPa	t_R h	$\epsilon_{r,R}$ %	Z %	$\dot{\epsilon}_{c,s}$ %/h	$t_{1,2}$ h	$t_{2,3}$ h
400	0.083	18	62	-	-	-
350	12.8	2	7	0.0974	1.0	6.8
345	10.0	7	5	0.1279	0.6	5.2
325	66.9	8	2	0.1238	3.6	50.9
304	390.9	-	-	0.00079	9.2	390.8
241	167.8	7	6	0.00474	12.3	139.7
193*	>3,630	-	-	0.0001	2,100	-

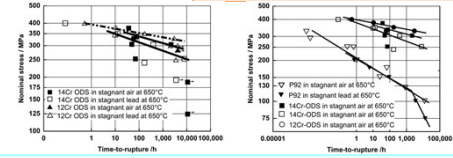
* - stopped

Table: Creep-to-rupture characteristics of the steel in stagnant air at 650°C

σ MPa	t_R h	$\epsilon_{r,R}$ %	Z %	$\dot{\epsilon}_{c,s}$ %/h	$t_{1,2}$ h	$t_{2,3}$ h
375	36.7	7	4	0.0396	1.4	35.8
337	76.8	7	5	0.0165	0.57	76.1
328	59.2	6	6	0.0150	3.6	59.0
305	49.3	7	4	0.0091	1.1	41.5
304	2,199.3	4	7	0.0002	287.2	2,197.3
253	70.4	7	6	0.0024	1.1	70.3
188*	>10,890	-	-	9.5·10 ⁻⁵	1.4	-
125*	>10,890	-	-	9.3·10 ⁻⁵	6.0	-

* the test is still running

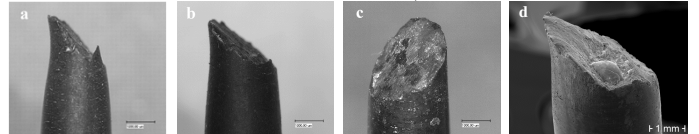
ODS and f/m P92 Steels



Stress-rupture and stress-secondary creep rate curves for the ODS and P92 steels in stagnant Pb and air

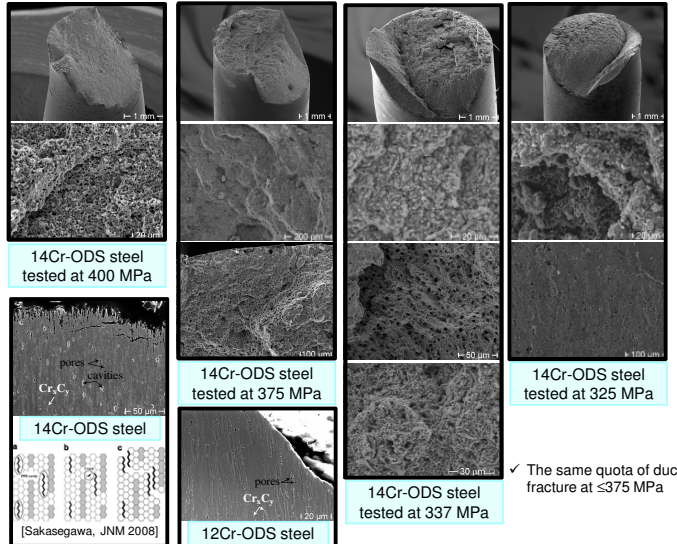
Post-Exposure Experiments

The higher stress, the higher $\epsilon_{c,R}$ and Z are.



12Cr-ODS steel tested at (a) 400 MPa, (b) 375 MPa, (c) 350 MPa, (d) 329 MPa.

Structures formed at different stresses:



14Cr-ODS steel tested at 400 MPa

14Cr-ODS steel tested at 375 MPa

14Cr-ODS steel tested at 325 MPa

14Cr-ODS steel tested at 337 MPa

12Cr-ODS steel

✓ The same quota of ductile fracture at ≤ 375 MPa

Summary

- The strength of 12Cr- and 14Cr-ODS steels is similar at 650°C and independent on the environment (Pb and air).
- The 12Cr-ODS steel features change in the deformation mechanism at ~ 330 MPa in Pb. In contrary, only one n that is very close in Pb and air was obtained for the 14Cr-ODS steel at < 375 MPa.
- Failure structure of the 14Cr-ODS steel is characterized by constant dimension of ductile area at ≤ 375 MPa ($\epsilon_{c,R}$ and Z are constant), while the 12Cr-ODS steel features growth of columnar transgranular structure in comparison to the ductile one with decrease of stress. Therefore, decrease of the secondary creep rate resulted in decrease of $\epsilon_{c,R}$ and Z.
- Diffusion degradation mechanism was observed in both ODS steels.

Acknowledgment

Funding by the EURATOM 7th Framework Programme within the cross-cutting project GETMAT (contract no. FP7-212175) is gratefully acknowledged.